

# A Trinal-Code Shifted Differential Chaos Shift Keying System

Xiangming Cai, Weikai Xu, *Member, IEEE*, Shaohua Hong, *Member, IEEE*, Lin Wang, *Senior Member, IEEE*

**Abstract**—In the differential chaos shift keying (DCSK) system, half of the symbol period is used to transmit the reference signal, resulting in the poor energy efficiency. The existing DCSK-based systems also inherit this disadvantage, restricting the development of DCSK-based systems significantly. To tackle this issue completely, we propose a trinal-code shifted differential chaos shift keying (TCS-DCSK) system, where information bits are solely transmitted by specific indices of Walsh codes and thus this system removes the reference signal. Comparison results of energy efficiency show that the TCS-DCSK system achieves higher energy efficiency in contrast to its competitors. In addition, we derive the bit error rate (BER) expressions of the TCS-DCSK system over additive white Gaussian noise (AWGN) and multipath Rayleigh fading channels. Finally, the BER performance of the TCS-DCSK system is compared to that of other systems. It is shown that the TCS-DCSK system can obtain considerable performance gain compared to other state-of-the-art chaotic communication systems.

**Index Terms**—Chaotic communications, differential chaos shift keying, energy efficiency, bit error rate (BER).

## I. INTRODUCTION

Chaotic communications have been widely studied in the past several decades [1]. As a representative of non-coherent schemes, the differential chaos shift keying (DCSK) system [2] has advantages of simple structure, removal of channel state information (CSI), without the need of chaos synchronization, resistance to multipath fading, thereby motivating researchers to fully exploit every potentials of DCSK-based schemes [3]. However, the DCSK system is inherently characterized by the transmitted-reference (TR) structure, i.e., half of symbol duration is used to transmit the non-information-bearing reference signal, lowering the data rate and energy efficiency.

To tackle this issue, lots of efforts have been devoted to designing high-data-rate-oriented chaotic communication systems. For example, Galias *et al.* proposed a quadrature chaos shift keying (QCSK) system [4], obtaining double data rate with the same consumption of bandwidth resource compared to the DCSK system. Then, the QCSK system was extended to its  $M$ -ary version in [5]. By introducing the code-shifted paradigm, a generalized code-shifted DCSK (GCS-DCSK) system [6] separates multiple information bearing signals by utilizing the orthogonality of Walsh codes. A multilevel code-shifted DCSK (MCS-DCSK) system was proposed in [7], where the received reference and information bearing signals

are averaged prior to correlation operations, mitigating the influence of noises. Moreover, an orthogonal multilevel DCSK (OM-DCSK) system [8] was proposed to enhance the data rate. A noise reduction DCSK (NR-DCSK) [9] system was proposed to enhance robustness by a moving average filter.

Recently, with the aid of the Walsh-codes-based  $M$ -ary modulation, a multilevel code-shifted  $M$ -ary DCSK (MCS-MDCSK) system [10] was proposed to achieve higher data rate and better BER performance. In addition, multiple reference signals are used in an MCS-DCSK system with reference diversity (MCS-DCSK-RD) [11] to realize the reference diversity. A discrete-cosine-spreading aided  $M$ -ary DCSK (DCS-MDCSK) [12] was proposed to achieve higher data rate without the penalty of BER performance. Note that many non-information-bearing signals of the DCS-MDCSK system are used as reference signals, thus lowering the energy efficiency. Furthermore, a code-index-modulation-based multicarrier  $M$ -ary DCSK (CIM-MC-MDCSK) system [13], [14] can obtain a higher data rate with the help of index modulation, multicarrier modulation and  $M$ -ary modulation. A dual-mode DCSK with index modulation (DM-DCSK-IM), configured with a pair of distinguishable modem-mode constellations, was proposed in [15]. Moreover, additional bits are transmitted by the indices of active time slots in the  $M$ -ary DCSK scheme with index modulation (IM-MCDSK) [16], thus obtaining a high data rate.

In brief, the aforementioned DCSK-based systems need to transmit one or more reference signals, which means part of transmitted energy is consumed by reference signals and this results in the poor energy efficiency. In order to solve this issue, we propose a trinal-code shifted differential chaos shift keying (TCS-DCSK) system. In this design, information bits are not directly transmitted by the traditional TR structure of DCSK-based systems, but by specific indices of Walsh codes. In this system, the reference signal is removed, thereby providing high energy efficiency. Then, the energy efficiency and system complexity of the TCS-DCSK system are analyzed. Compared to other chaotic communication systems, the TCS-DCSK system can obtain higher energy efficiency at the expense of system complexity. Furthermore, we derive the theoretical BERs for the TCS-DCSK system over AWGN and multipath fading channels, which are checked by computer simulations. Simulation results show that the TCS-DCSK system can achieve better BER performance than other up-to-date chaotic communication systems.

Section II introduces the system model of the TCS-DCSK system. In Section III, the theoretical BER expressions of the TCS-DCSK system are given. Simulation results are shown in Section IV. Finally, Section V concludes our findings.

This work was supported in part by the National Natural Science Foundation of China under Grant No. 61671395 and 61871337.

Xiangming Cai, Weikai Xu, Shaohua Hong and Lin Wang are with the Department of Information and Communication Engineering, Xiamen University, Xiamen, P. R. China. (e-mail: samson0102@qq.com, xweikai@xmu.edu.cn, hongsh@xmu.edu.cn, wanglin@xmu.edu.cn).

## II. THE TCS-DCSK SYSTEM

### A. The Transmitter

The block diagram of the TCS-DCSK transmitter is given in Fig. 1(a). The overall transmitted bits are divided into three equal parts, and each part includes  $n$  bits. Specifically, the first  $n$  bits  $\mathbf{a} = \{a_1, a_2, \dots, a_n\}$  are used to select a Walsh code  $\mathbf{w}_g = [w_{g,1}, w_{g,2}, \dots, w_{g,N}]$ ,  $g \in \partial$  to spread the chaotic signal, where  $\partial = \{1, 2, \dots, N\}$  and  $N = 2^n$  denotes the order of Walsh codes. Similarly, the remaining  $2n$  bits  $\mathbf{b} = \{b_1, b_2, \dots, b_n\}$  and  $\mathbf{d} = \{d_1, d_2, \dots, d_n\}$  are arranged to choose Walsh codes  $\mathbf{w}_p, p \in \partial$  and  $\mathbf{w}_q, q \in \partial$ , respectively. The indices of Walsh codes  $g, p, q$  can be determined by  $g = \mathbb{M}(\mathbf{a}) + 1$ ,  $p = \mathbb{M}(\mathbf{b}) + 1$  and  $q = \mathbb{M}(\mathbf{d}) + 1$ , respectively, where  $\mathbb{M}(\cdot)$  is the binary-to-decimal conversion function. Note that the above three selected Walsh codes can be the same, partially same or different, which is determined by the information bits  $\mathbf{a}$ ,  $\mathbf{b}$  and  $\mathbf{d}$ . Clearly, since information bits are transmitted by specific indices of selected Walsh codes implicitly, the reference signal is removed. According to Fig. 1(a), the transmitted signal is given as

$$s(t) = c_a(t) \cos(2\pi f_0 t) - \frac{\sqrt{2}}{2} [c_b(t) + c_d(t)] \sin(2\pi f_0 t), \quad (1)$$

where  $c_a(t) = \sum_{k=1}^{\beta} (\mathbf{w}_g \otimes \mathbf{c}_x)_k h_p(t - kT_c)$ . In addition to this, one has  $c_b(t) = \sum_{k=1}^{\beta} (\mathbf{w}_p \otimes \mathbf{c}_x)_k h_p(t - kT_c)$  and  $c_d(t) = \sum_{k=1}^{\beta} (\mathbf{w}_q \otimes \mathbf{c}_y)_k h_p(t - kT_c)$ .  $f_0$  is the frequency of the sinusoidal carrier. Moreover,  $\mathbf{c}_x = [c_{x,1}, c_{x,2}, \dots, c_{x,\theta}]$  is a  $\theta$ -length chaotic sequence, generated by the logistic map  $c_{k+1} = 1 - 2c_k^2$ ,  $k = 1, 2, \dots$ . Then, signal  $\mathbf{c}_x$  is loaded into the Hilbert filter to obtain its orthogonal signal  $\mathbf{c}_y$ . After that, the obtained  $\mathbf{c}_x$  and  $\mathbf{c}_y$  are multiplied by the corresponding Walsh codes using the Kronecker product  $\otimes$ . Here,  $(\cdot)_k$  denotes the  $k^{\text{th}}$  sampling value, while  $T_c$  is chip interval of the chaotic sequence. Furthermore,  $h_p(t)$  is the normalized pulse response of a square-root-raised-cosine filter. Here, we define a symbol duration as the spreading factor, namely  $\beta = N\theta$ .

### B. The Receiver

After the transmitted signal passes through the multipath fading channel and then the resultant signal is polluted by a Gaussian noise  $n(t)$  with zero mean and power spectral density of  $N_0/2$ , the received signal can be expressed as

$$r(t) = \sum_{l=1}^L \lambda_l s(t - \tau_l) + n(t), \quad (2)$$

where  $L$  is the number of paths.  $\lambda_l$  and  $\tau_l$  are the channel coefficient and the corresponding path delay. Fig. 1(b) shows the TCS-DCSK receiver. The simple synchronization of Walsh codes is needed at the receiver. After the received signal is multiplied by different carrier components and then sent to the corresponding matched filters, the resultant signals are sampled with time interval  $T_c$ . After that, the discrete signal  $\mathbf{r}_x$  corresponding to the cosine branch is loaded into the Hilbert filter to get its orthogonal signal  $\mathbf{r}_y$ . In addition,  $\mathbf{r}_m$  is the discrete signal corresponding to the sine branch. Subsequently, signals  $\mathbf{r}_x$ ,  $\mathbf{r}_y$  and  $\mathbf{r}_m$  are multiplied by  $\mathbf{J}$  using the Hadamard product  $\odot$ , where  $\mathbf{J} = \mathbf{w}_i \otimes \mathbf{1}_{1 \times \theta}$ ,  $i \in \partial$  is an

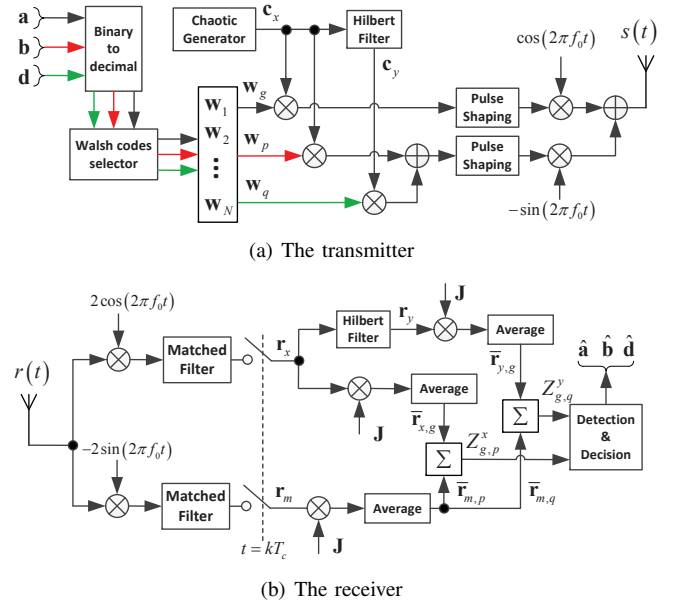


Fig. 1. Block diagram of the TCS-DCSK system.

extended Walsh code and  $\mathbf{w}_i = [w_{i,1}, w_{i,2}, \dots, w_{i,N}]$ . Then the obtained signal  $\mathbf{r}_x$  is processed by the average operation, yielding  $\bar{\mathbf{r}}_{x,g} = \frac{1}{N} \sum_{n=1}^N w_{g,n} \mathbf{r}_x[(n-1)\theta + 1 : n\theta]$ , where  $\mathbf{r}_x[(n-1)\theta + 1 : n\theta]$  is the  $\{(n-1)\theta + 1\}^{\text{th}}$  to  $(n\theta)^{\text{th}}$  element of  $\mathbf{r}_x$ . Similarly, other signals  $\bar{\mathbf{r}}_{y,g}$ ,  $\bar{\mathbf{r}}_{m,p}$  and  $\bar{\mathbf{r}}_{m,q}$  can be obtained. The resultant signals  $\bar{\mathbf{r}}_{x,g}$  and  $\bar{\mathbf{r}}_{y,g}$  are correlated with  $\bar{\mathbf{r}}_{m,k}$  to obtain decision variables  $Z_{g,p}^x = \bar{\mathbf{r}}_{x,g} [\bar{\mathbf{r}}_{m,p}]^T$  and  $Z_{g,q}^y = \bar{\mathbf{r}}_{y,g} [\bar{\mathbf{r}}_{m,q}]^T$ , where  $[\cdot]^T$  is the transposition. Finally, the indices of Walsh codes can be determined by

$$(\hat{g}, \hat{p}) = \arg \max \{|Z_{g,p}^x|\}, \quad (\hat{g}, \hat{q}) = \arg \max \{|Z_{g,q}^y|\}, \quad (3)$$

where  $\hat{g}$ ,  $\hat{p}$  and  $\hat{q}$  denote the estimated indices of Walsh codes which are used to transmit  $\mathbf{a}$ ,  $\mathbf{b}$  and  $\mathbf{d}$ , respectively. After transforming the obtained indices into binary bits, the receiver retrieves the initial information bits.

### C. Energy Efficiency and System Complexity

In this subsection, the energy efficiency and system complexity of the TCS-DCSK system are analyzed to underline its advantages. Here, the energy efficiency is defined by the overall transmitted bits per energy in a symbol. Clearly, the energy efficiency can be calculated by carrying out the reciprocal operation of bit energy, i.e.,  $EE = \frac{1}{E_b}$ . Considering the signal structure of the TCS-DCSK system, the bit energy of the TCS-DCSK system is  $E_b = \frac{1}{3 \log_2 N} 2 \sum_{k=1}^{\beta} c_k^2$ . When  $\sum_{k=1}^{\beta} c_k^2 = 1$ , namely the energy of chaotic signal is normalized, the energy efficiency of the TCS-DCSK system is given by  $\frac{3}{2} \log_2 N$ . In addition, the bit energy and energy efficiency of other chaotic communication systems can be computed in a similar manner. As observed in Table I, the TCS-DCSK system can obtain better energy efficiency than its competitors, because the TCS-DCSK system removes the reference signal. However, other DCSK-based systems need one or more reference signals, resulting in the poor energy efficiency.

TABLE I  
BIT ENERGY, ENERGY EFFICIENCY AND SYSTEM COMPLEXITY OF TCS-DCSK AND OTHER CHAOTIC COMMUNICATION SYSTEMS

Systems	TCS-DCSK	MCS-DCSK	MCS-MDCSK	OM-DCSK	MCS-DCSK-RD
Bit Energy	$\frac{2 \sum_{k=1}^{\beta} c_k^2}{3 \log_2 N}$	$\frac{[(N-1)+1] \sum_{k=1}^{\beta} c_k^2}{N-1}$	$\frac{(\frac{N-2}{2}+1) \sum_{k=1}^{\beta} c_k^2}{\frac{N-2}{2} \log_2 M}$	$\frac{3 \sum_{k=1}^{\beta} c_k^2}{\log_2(2N)}$	$\frac{(N_r+N_i) \sum_{k=1}^{\beta} c_k^2}{N_i}$
Energy Efficiency	$\frac{3}{2} \log_2 N$	$\frac{N-1}{N}$	$\frac{(N-2) \log_2 M}{N}$	$\frac{\log_2(2N)}{3}$	$\frac{N_i}{N_r+N_i}$
Complexity	$3 + 2N^2$	$2(N-1)$	$2(N-2)$	$4N$	$2N_i$

†  $M$  is the modulation order of the MCS-MDCSK system. In the MCS-DCSK-RD system,  $N_r$  and  $N_i$  are the number of reference and information bearing signals, respectively.

Here, we use the total number of spreading/despreading operations in the transceiver to evaluate system complexity. According to the TCS-DCSK transceiver in Fig. 1, the number of spreading operations in the transmitter is equal to 3, while the receiver requires  $2N^2$  despreading operations. Therefore, complexity of the TCS-DCSK system is  $3 + 2N^2$ . Table I shows the system complexity of other chaotic communication systems. Since information bits of the TCS-DCSK system are transmitted with the aid of indices of Walsh codes, many despreading operations are needed to determine the selected Walsh codes and then information bits are retrieved by specific indices of the selected codes. Therefore, system complexity of the TCS-DCSK system is much higher than its competitors.

### III. PERFORMANCE ANALYSIS

The transmitted bits are carried by indices of Walsh codes implicitly, so that the TCS-DCSK receiver needs to perform correlation  $N^2$  times to recover bits  $\mathbf{a}$  and  $\mathbf{b}$  from signals  $\bar{\mathbf{r}}_{x,g}$  and  $\bar{\mathbf{r}}_{m,p}$ . Since the decision variable  $Z_{g,p}^x$  is independent and symmetric to  $Z_{g,q}^y$ , we consider  $Z_{g,p}^x$  for brevity. Signal  $\bar{\mathbf{r}}_{x,g} = \frac{1}{N} \sum_{n=1}^N w_{g,n} \mathbf{r}_x[(n-1)\theta + 1 : n\theta]$  is simplified as

$$\bar{\mathbf{r}}_{x,g} = \frac{1}{N} \sum_{n=1}^N w_{g,n} (w_{g',n} \sum_{l=1}^L \lambda_l \mathbf{c}_{x,\tau_l} + \mathbf{n}_x) \quad (4)$$

$$= \begin{cases} \sum_{l=1}^L \lambda_l \mathbf{c}_{x,\tau_l} + \tilde{\mathbf{n}}_x = \mathbf{A}_1, g' = g \\ \tilde{\mathbf{n}}_x = \mathbf{A}_2, g' \neq g \end{cases}$$

where  $\tilde{\mathbf{n}}_x = \frac{1}{N} \sum_{n=1}^N w_{g,n} \mathbf{n}_x$  is an AWGN with zero mean and  $N_0/2N$  variance. Similarly,  $\bar{\mathbf{r}}_{m,p}$  is rewritten as  $\bar{\mathbf{r}}_{m,k} = \frac{1}{N} \sum_{n=1}^N w_{k,n} \mathbf{r}_m[(n-1)\theta + 1 : n\theta]$ , which can be classified into two different cases,  $i = j$  and  $i \neq j$ , where  $i$  and  $j$  are indices of Walsh codes used to spread  $\mathbf{c}_x$  and  $\mathbf{c}_y$  within the sine branch, respectively. When  $i = j$ ,  $\bar{\mathbf{r}}_{m,k}$  can be given as

$$\bar{\mathbf{r}}_{m,k} = \frac{1}{N} \sum_{n=1}^N w_{k,n} w_{i,n} \left[ \frac{\sqrt{2}}{2} \sum_{l=1}^L \lambda_l (\mathbf{c}_{x,\tau_l} + \mathbf{c}_{y,\tau_l}) + \mathbf{n}_m \right]$$

$$= \begin{cases} \frac{\sqrt{2}}{2} \sum_{l=1}^L \lambda_l (\mathbf{c}_{x,\tau_l} + \mathbf{c}_{y,\tau_l}) + \tilde{\mathbf{n}}_m = \mathbf{B}_1, i = k \\ \tilde{\mathbf{n}}_m = \mathbf{B}_2, i \neq k \end{cases} \quad (5)$$

TABLE II  
MEANS AND VARIANCES OF DECISION VARIABLE  $Z_{g,p}^x$  WHEN  $i = j$ .

$Z_{g,p}^x$	$Z_1$	$Z_2$	$Z_3$	$Z_4$
mean	$\mu$	0	0	0
variance	$\sigma_1^2$	$\sigma_2^2$	$\sigma_2^2$	$\sigma_3^2$

† Note that  $Z_1 = \mathbf{A}_1(\mathbf{B}_1)^T$ ,  $Z_2 = \mathbf{A}_1(\mathbf{B}_2)^T$ ,  $Z_3 = \mathbf{A}_2(\mathbf{B}_1)^T$  and  $Z_4 = \mathbf{A}_2(\mathbf{B}_2)^T$ . In addition,  $\sigma_1^2 = \sum_{l=1}^L \lambda_l^2 \frac{2E_s N_0}{4N^2} + \theta \frac{N_0^2}{4N^2}$ ,  $\sigma_2^2 = \sum_{l=1}^L \lambda_l^2 \frac{E_s N_0}{4N^2} + \theta \frac{N_0^2}{4N^2}$  and  $\sigma_3^2 = \theta \frac{N_0^2}{4N^2}$ .

where  $\tilde{\mathbf{n}}_m = \frac{1}{N} \sum_{n=1}^N w_{k,n} \mathbf{n}_m$  is the AWGN with the same mean and variance as  $\tilde{\mathbf{n}}_x$ . Therefore,  $Z_1 = \mathbf{A}_1(\mathbf{B}_1)^T$  is

$$Z_1 = \left[ \sum_{l=1}^L \lambda_l \mathbf{c}_{x,\tau_l} + \tilde{\mathbf{n}}_x \right] \left[ \frac{\sqrt{2}}{2} \sum_{l=1}^L \lambda_l (\mathbf{c}_{x,\tau_l} + \mathbf{c}_{y,\tau_l}) + \tilde{\mathbf{n}}_m \right]^T. \quad (6)$$

Therefore, the mean and variance of  $Z_1$  are computed by

$$\mathbb{E}[Z_1] = \sum_{l=1}^L \lambda_l^2 \frac{\sqrt{2}E_s}{4N} = \mu, \quad (7)$$

$$\text{Var}[Z_1] = \sum_{l=1}^L \lambda_l^2 \frac{2E_s N_0}{4N^2} + \theta \frac{N_0^2}{4N^2} = \sigma_1^2, \quad (8)$$

where  $E_s = 2N\theta\mathbb{E}[c_j^2]$  is the symbol energy of the TCS-DCSK system and  $\mathbb{E}[c_j^2]$  is the energy of the chaotic chip. The symbol signal to noise ratio (SNR) is given as  $\gamma_s = \sum_{l=1}^L \lambda_l^2 \frac{E_s}{N_0}$ . Table II gives the means and variances of other cases for the decision variable  $Z_{g,p}^x$ . Since the decision variable  $Z_{g,p}^x$  can be regarded as a Gaussian variable, the error probability for estimating the current symbol is calculated by

$$P_1 = 1 - \int_0^\infty \Pr(|Z_2| < z, \dots, |Z_4| < z, |z| = |Z_1|) f(z) dz$$

$$= \int_0^\infty \left\{ 1 - [F_{|Z_2|}(z)]^{N-1} [F_{|Z_3|}(z)]^{N-1} \right. \\ \left. \times [F_{|Z_4|}(z)]^{(N-1)^2} \right\} f_{|Z_1|}(z) dz, \quad (9)$$

where  $f_{|Z_i|}(z)$  and  $F_{|Z_i|}(z)$ ,  $i = 2, 3, 4$  denote the probability density function (PDF) of  $|Z_i|$  and the cumulative distribution functions (CDF) of  $|Z_i|$ ,  $i = 2, 3, 4$ , respectively, given as  $f_{|Z_1|}(z) = \frac{1}{\sqrt{2\pi\sigma_1^2}} [\exp(-\frac{(z-\mu)^2}{2\sigma_1^2}) + \exp(-\frac{(z+\mu)^2}{2\sigma_1^2})]$ ,  $F_{|Z_2|}(z) = F_{|Z_3|}(z) = \text{erf}(\frac{z}{\sqrt{2\sigma_2^2}})$  and  $F_{|Z_4|}(z) = \text{erf}(\frac{z}{\sqrt{2\sigma_3^2}})$ , where  $\text{erf}(z) = \frac{2}{\sqrt{\pi}} \int_0^z e^{-t^2} dt$ ,  $z \geq 0$  is the error function.

TABLE III  
THE MEANS AND VARIANCES OF DECISION VARIABLE  $Z_{g,p}^x$  IN THE CASE OF  $i \neq j$ .

$Z_{g,p}^x$	$\mathbf{A}_1(\mathbf{D}_1)^T = Y_1$	$\mathbf{A}_1(\mathbf{D}_2)^T = Y_2$	$\mathbf{A}_1(\mathbf{D}_3)^T = Y_3$	$\mathbf{A}_2(\mathbf{D}_1)^T = Y_4$	$\mathbf{A}_2(\mathbf{D}_2)^T = Y_5$	$\mathbf{A}_2(\mathbf{D}_3)^T = Y_6$
mean	$\mu$	0	0	0	0	0
variance	$\sigma_4^2$	$\sigma_4^2$	$\sigma_2^2$	$\sigma_5^2$	$\sigma_5^2$	$\sigma_3^2$

<sup>†</sup> Note that  $\sigma_4^2 = \sum_{l=1}^L \lambda_l^2 \frac{3E_s N_0}{8N^2} + \theta \frac{N_0^2}{4N^2}$ ,  $\sigma_2^2 = \sum_{l=1}^L \lambda_l^2 \frac{E_s N_0}{4N^2} + \theta \frac{N_0^2}{4N^2}$ ,  $\sigma_5^2 = \sum_{l=1}^L \lambda_l^2 \frac{E_s N_0}{8N^2} + \theta \frac{N_0^2}{4N^2}$  and  $\sigma_3^2 = \theta \frac{N_0^2}{4N^2}$ .

Regarding the case of  $i \neq j$ ,  $\bar{\mathbf{r}}_{m,k}$  is given as

$$\bar{\mathbf{r}}_{m,k} = \frac{1}{N} \sum_{n=1}^N w_{k,n} \left[ \frac{\sqrt{2}}{2} \sum_{l=1}^L \lambda_l (w_{i,n} \mathbf{c}_{x,\tau_l} + w_{j,n} \mathbf{c}_{y,\tau_l}) + \mathbf{n}_m \right]$$

$$= \begin{cases} \frac{\sqrt{2}}{2} \sum_{l=1}^L \lambda_l \mathbf{c}_{x,\tau_l} + \tilde{\mathbf{n}}_m = \mathbf{D}_1, i = k, j \neq k \\ \frac{\sqrt{2}}{2} \sum_{l=1}^L \lambda_l \mathbf{c}_{y,\tau_l} + \tilde{\mathbf{n}}_m = \mathbf{D}_2, i \neq k, j = k \\ \tilde{\mathbf{n}}_m = \mathbf{D}_3, i \neq k, j \neq k \end{cases} \quad (10)$$

In this case, the means and variances of  $Z_{g,p}^x$  are summarized in Table III. Similar to the case of  $i = j$ , the incorrect detection probability of the current symbol is computed by

$$P_2 = 1 - \int_0^\infty \Pr(|Y_2| < z, \dots, |Y_6| < z | z = |Y_1|) f(z) dz$$

$$= \int_0^\infty \left\{ 1 - [F_{|Y_2|}(z)] [F_{|Y_3|}(z)]^{N-2} [F_{|Y_4|}(z)]^{N-1} \right.$$

$$\left. \times [F_{|Y_5|}(z)]^{N-1} [F_{|Y_6|}(z)]^{(N-1)(N-2)} \right\} f_{|Y_1|}(z) dz, \quad (11)$$

where  $f_{|Y_1|}(z) = \frac{1}{\sqrt{2\pi\sigma_4^2}} [\exp(-\frac{(z-\mu)^2}{2\sigma_4^2}) + \exp(-\frac{(z+\mu)^2}{2\sigma_4^2})]$ ,  $F_{|Y_2|}(z) = \text{erf}(\frac{z}{\sqrt{2\sigma_4^2}})$ ,  $F_{|Y_3|}(z) = \text{erf}(\frac{z}{\sqrt{2\sigma_2^2}})$ ,  $F_{|Y_4|}(z) = \text{erf}(\frac{z}{\sqrt{2\sigma_5^2}})$  and  $F_{|Y_6|}(z) = \text{erf}(\frac{z}{\sqrt{2\sigma_3^2}})$ .

Assuming that the information bits are transmitted equiprobably, the BER of the TCS-DCSK system can be obtained by

$$P_T = \frac{2(2n-1)}{2^{2n}-1} \left( \frac{1}{2^n} P_1 + \frac{2^n-1}{2^n} P_2 \right). \quad (12)$$

Considering an  $L$ -paths dissimilar Rayleigh fading channel, according to [17], the PDF of the symbol-SNR  $\gamma_s$  is  $f(\gamma_s) = \sum_{l=1}^L [\frac{1}{\bar{\gamma}_l} (\prod_{j=1, j \neq l}^L \frac{\bar{\gamma}_l}{\bar{\gamma}_l - \bar{\gamma}_j}) \exp(-\frac{\gamma_s}{\bar{\gamma}_l})]$ , where  $\bar{\gamma}_l$  denotes the average of the instantaneous SNR measured in the  $l^{\text{th}}$  channel. Therefore, the averaged BER of the TCS-DCSK system over multipath Rayleigh fading channel is obtained after integrating  $\bar{P}_T = \int_0^\infty P_T \cdot f(\gamma_s) d\gamma_s$ .

#### IV. NUMERICAL RESULTS AND DISCUSSIONS

In simulations, a three-paths Rayleigh fading channel with power factors  $E(\lambda_1^2) = 1/2$ ,  $E(\lambda_2^2) = 1/3$ ,  $E(\lambda_3^2) = 1/6$  and channel delays  $\tau_1 = 0$ ,  $\tau_2 = T_c$ ,  $\tau_3 = 5T_c$  is used. Fig. 2 shows the BER performance of the TCS-DCSK system with different  $\theta$ . Clearly, simulation results match the theoretical ones well. When  $\theta$  increases, the BER performance of the TCS-DCSK system becomes worse. In Fig. 3, the TCS-DCSK system with  $N = 32$  performs almost 4dB performance gain better than that of  $N = 4$  at the BER level of  $10^{-5}$  over the

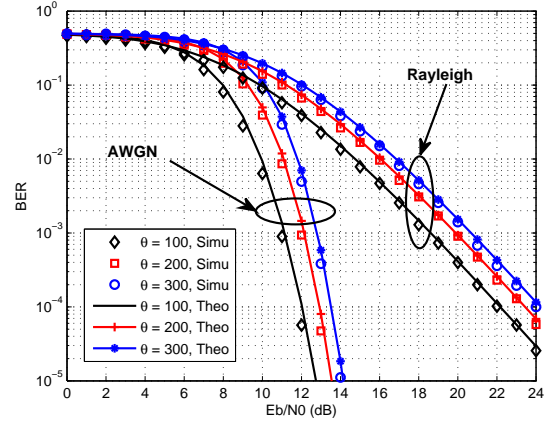


Fig. 2. BER performance of the TCS-DCSK system over AWGN and multipath Rayleigh fading channels.  $N = 8$  and  $\theta = 100, 200, 300$ .

AWGN channel. It is mainly due to that a larger  $N$  means more bits are transmitted by indices of Walsh codes with the same energy consumption, improving the BER performance.

In Fig. 4, the BER performance of the TCS-DCSK system is compared to that of its competitors. In all systems, the number of transmitted bits per symbol is  $\Gamma = 12$  and the order of Walsh codes  $N$  is 16. The MCS-DCSK-RD system has 2 reference signal. The DCS-DCSK system has 2 orthogonal chaotic signals, and the length of discrete-cosine-spreading codes is 4. The modulation order of the MCS-MDCSK system is 4. Clearly, the TCS-DCSK system can obtain about 3dB gain over MCS-DCSK-RD and MCS-MDCSK systems and about 4dB gain over the DCS-DCSK system at the BER level of  $10^{-5}$  in the AWGN channel. However, the BER performance of the TCS-DCSK system is slightly inferior to its competitors when  $E_b/N_0 < 5$ dB. This is due to the error probability of index detection is large when  $E_b/N_0$  is small.

Fig. 5 shows the BERs of TCS-DCSK and CIM-MC-MDCSK systems. The modulation order of the CIM-MC-MDCSK system is 4. The TCS-DCSK system outperforms the CIM-MC-MDCSK system and the gain is 3 to 6dB at the BER of  $10^{-5}$  in the AWGN channel. It is due to the TCS-DCSK system only transmits indexed bits while the CIM-MC-MDCSK system conveys physically modulated bits in addition to indexed bits. In Fig. 6, the BER performance of the TCS-DCSK system is similar to that of the IM-MDCSK system in the AWGN channel, but worse than the IM-MDCSK system in the multipath Rayleigh fading channel with large delays. Moreover, the TCS-DCSK system reaches its error floor more quickly than its competitors in the channel with large delays.

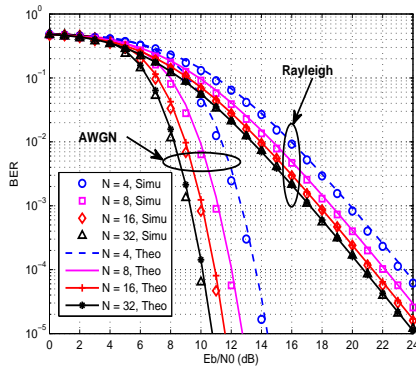


Fig. 3. BER performance of the TCS-DCSK system.  $\theta = 100$  and  $N = 4, 8, 16, 32$ .

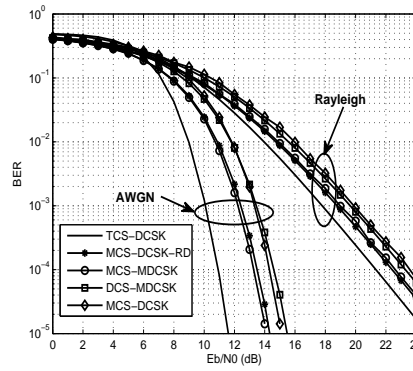


Fig. 4. BER performance of TCS-DCSK and other chaotic communication systems.  $\theta = 100$ .

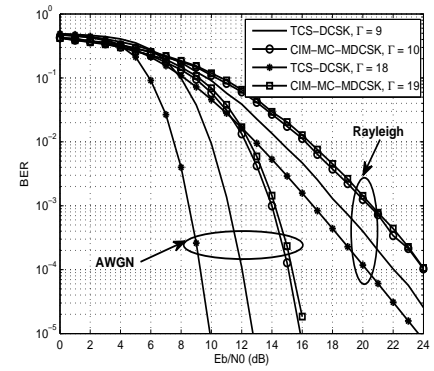


Fig. 5. BER performance of TCS-DCSK and CIM-MC-MDCSK systems.  $\theta = 100$ .

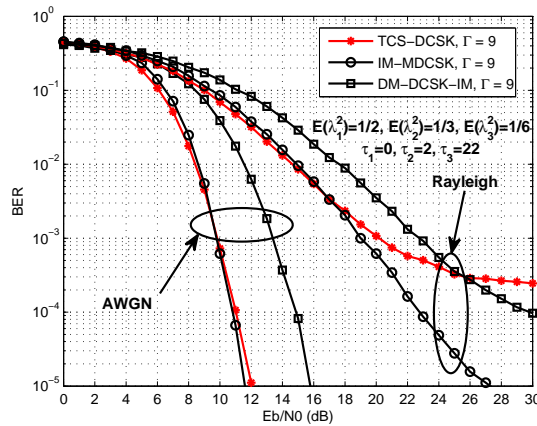


Fig. 6. BER performance of TCS-DCSK, IM-MDCSK and DM-DCSK-IM systems.  $\theta = 40$ . The modulation order of the IM-MDCSK system is 4.

## V. CONCLUSION

In this paper, we propose a trinal-code shifted differential chaos shift keying system, aiming at improving the energy efficiency and BER performance of traditional DCSK-based systems. The information bits of the TCS-DCSK system are transmitted without the need of the reference signal, thereby improving the energy efficiency significantly. Specifically, indices of Walsh codes are regarded as a dimension to transmit information bits, enhancing the BER performance. In addition, theoretical analysis is performed for the TCS-DCSK system, which is confirmed by computer simulations. Moreover, simulation results show that, although the TCS-DCSK system reaches error floor of BER performance more quickly than IM-MDCSK and DM-DCSK-IM systems, the TCS-DCSK system have stronger robustness than other DCSK-based systems over AWGN and multipath Rayleigh fading channel with small delays. Facing severe challenges of limited energy resource and harsh channel environment in future communication, the proposed TCS-DCSK system is a promising solution.

## REFERENCES

[1] G. Kaddoum, "Wireless chaos-based communication systems: A comprehensive survey," *IEEE Access*, vol. 4, pp. 2621-2648, 2016.

[2] G. Kolumbán, G. K. Vizvári, W. Schwarz, and A. Abel, "Differential chaos shift keying: A robust coding for chaos communication," in *Proc. Nonlinear Dyn. Electron. Syst.*, Seville, Spain, Jun. 1996, pp. 92-97.

[3] Y. Fang, G. Han, P. Chen, F. C. M. Lau, G. Chen, and L. Wang, "A survey on DCSK-based communication systems and their application to UWB scenarios," *IEEE Commun. Surveys Tuts.*, vol. 18, no. 3, pp. 1804-1837, 3rd Quart., 2016.

[4] Z. Galias and G. M. Maggio, "Quadrature chaos-shift keying: Theory and performance analysis," *IEEE Trans. Circuits Syst. I, Fundam. Theory Appl.*, vol. 48, no. 12, pp. 1510-1519, Dec. 2001.

[5] L. Wang, G. Cai, and G. Chen, "Design and performance analysis of a new multiresolution  $M$ -ary differential chaos shift keying communication system," *IEEE Trans. Wireless Commun.*, vol. 14, no. 9, pp. 5197-5208, Sept. 2015.

[6] W. Xu, L. Wang, and G. Kolumbán, "A new data rate adaption communication scheme for code-shifted differential chaos shift keying modulation," *Int. J. Bifurcation Chaos*, vol. 22, no. 8, pp. 1-8, 2012.

[7] T. Huang, L. Wang, W. Xu, and F. C. M. Lau, "Multilevel code-shifted differential-chaos-shift-keying system," *IET Commun.*, vol. 10, no. 10, pp. 1189-1195, Jul. 2016.

[8] H. Yang, W. K. S. Tang, G. Chen, and G.-P. Jiang, "System design and performance analysis of orthogonal multi-level differential chaos shift keying modulation scheme," *IEEE Trans. Circuits Syst. I, Reg. Papers*, vol. 63, no. 1, pp. 146-156, Jan. 2016.

[9] G. Kaddoum and E. Soujeri, "NR-DCSK: A noise reduction differential chaos shift keying system," *IEEE Trans. Circuits Syst., II, Exp. Briefs*, vol. 63, no. 7, pp. 648-652, Jul. 2016.

[10] X. Cai, W. Xu, R. Zhang and L. Wang, "A multilevel code shifted differential chaos shift keying system with  $M$ -ary modulation," *IEEE Trans. Circuits Syst., II, Exp. Briefs*, vol. 66, no. 8, pp. 1451-1455, Aug. 2019.

[11] Y. Lu, M. Miao, L. Wang and W. Xu, "A multilevel code-shifted differential chaos shift keying system with reference diversity," *IEEE Trans. Circuits Syst., II, Exp. Briefs*, doi: 10.1109/TCSII.2020.2964883.

[12] Z. Chen, L. Zhang and Z. Wu, "High data rate discrete-cosine-spreading aided  $M$ -ary differential chaos shift keying scheme with low PAPR," *IEEE Trans. Circuits Syst., II, Exp. Briefs*, doi: 10.1109/TCSII.2020.2980738.

[13] G. Cai, Y. Fang, J. Wen, S. Mumtaz, Y. Song and V. Frascolla, "Multi-carrier  $M$ -ary DCSK system with code index modulation: An efficient solution for chaotic communications," *IEEE J. Sel. Topics Signal Process.*, vol. 13, no. 6, pp. 1375-1386, Oct. 2019.

[14] G. Cai, Y. Fang, P. Chen, G. Han, G. Cai and Y. Song, "Design of a MISO-SWIPT-aided code-index modulated multi-carrier M-DCSK system for e-Health IoT," *IEEE J. Sel. Areas Commun.*, doi: 10.1109/ISAC.2020.3020603.

[15] X. Cai, W. Xu, S. Hong and L. Wang, "Dual-mode differential chaos shift keying with index modulation," *IEEE Trans. Commun.*, vol. 67, no. 9, pp. 6099-6111, Sept. 2019.

[16] X. Cai, W. Xu, M. Miao and L. Wang, "Design and performance analysis of a new  $M$ -ary differential chaos shift keying with index modulation," *IEEE Trans. Wireless Commun.*, vol. 19, no. 2, pp. 846-858, Feb. 2020.

[17] J. G. Proakis and M. Salehi, *Digital Communications*. New York, NY, USA: McGraw-Hill, 2007.